High-resolution computational fluid dynamics modelling of suspended shellfish structures

S. Delaux, C. L. Stevens, S. Popinet

Noname manuscript No.
(will be inserted by the editor)

High-Resolution Computational Fluid Dynamics Modelling of Suspended Shellfish Structures

S. Delaux · C. L. Stevens · S. Popinet

Received: date / Accepted: date

Abstract Aquaculture structures are responsible for flow disturbances that extend over a large range of scales. In the case of shellfish aquaculture, those scales extend from the size of an individual shellfish to the size of a whole farm with intermediate scales being the size of a shellfish structure or of a block of shellfish structures. The influence of block spacing and angle is investigated by the mean of a 2D high resolution computational fluid dynamics model. Block angle is found to be the main relevant parameter controlling to a large extent the mixing generated by the shellfish structures. Strong sensitivity is found for small angles. Nevertheless, it is shown that for a limited number of blocks, upstream turbulence still dominates the degree of the total mixing within the farm, and that total flow reduction is little affected by the orientation of the blocks. A simple analytical model is presented that predicts most of the numerical results.

Keywords Musselfarm, long-lines, drag, mixing, 2D turbulence, computational fluid dynamics

1 Introduction

Shellfish aquaculture in coastal waters involves exposing juvenile-seeded structures to nutrient-laden flows. Thus it holds a unique place among marine aquaculture techniques in that it is relatively low impact in terms of injection of nutrients into the local environment. However, it does require a large farmed area relative to the value of the crop produced. A consequence of this is that large farms, which enable large flow disturbances, are required to provide sufficient economic returns [Grant and Bacher(2001)]. These disturbances are not necessarily deleterious to the local environment, especially in areas of complex topography where the flow is already highly variable [Stevens et al(2008)]. However, farms will absorb nutrients and so generate a wake of nutrient-depleted fluid [C. A. Pilditch and Bryan(2001)]. Furthermore the effect of the farm will be to slow the flow within the farm and modify the local flow patterns [Plew et al(2005)].

National Institute of Water and Atmospheric Research, Greta Point, Private Bag 14901, Wellington, New Zealand E-mail: c.stevens@niwa.co.nz, Phone: +64 4 386 0476, Fax: +64 4 386 2153

This then impacts the distribution of relatively fast-sinking faeces and pseudo-faeces [Hartstein and Stevens(2005), Giles and Pilditch(2004)] and may have consequences for the environment as well as for the productivity of the farms [C. A. Pilditch and Bryan(2001)].

Farm structures are typically developed as rafts [Boyd and Heasman(1998), Blanco et al(1996)] or long-lines [Stevens et al(2008)]. The most popular method for green mussel (*Perna canaliculus*) aquaculture in New Zealand is the long-line technique and this is the focus here although aspects of the work will likely be applicable to raft culture. Long-line farms of up to 80 000 m^2 are made of a layout of farm blocks, each of them typically made of 5 to 15 long-lines. These long-lines, usually around 120 meters long, consist of two parallel "backbone" ropes supported by buoys and attached at both ends to anchor blocks either ballasted or screwed into the seabed (Figure 1). This structure is used to suspend a spat-laden culture rope forming loops (droppers) from sea-surface to 10 to 15 meters deep, sometimes more, depending on the depth, so that the culture rope stays clear of the sea bed. Whereas the orientation of the farm blocks can be variable, all blocks are made of parallel long-lines spaced at least 15-80 meters apart to allow vessel access.

When planning and assessing future farm development there is a need to represent the drag imparted by this distributed structure on the fluid. This enables quantification of the influence and impact of a single farm and also gauges the combined effect of several farms. While it is clearly important to resolve the correct functionality of the drag coefficient [Plew(2005), Plew(2009)], it is possible that there is just as much influence of farm arrangement on farm-scale flow. The present study uses two-dimensional high-resolution numerical techniques to evaluate the influence of several key farm arrangement parameters including angle of farm to the flow and spacing between blocks.

Flows past mussel farms are highly multi-scale [Stevens et al(2008)], with the three main relevant scales being those of a dropper, of a farm block and of the whole farm. All scales cannot be readily looked at simultaneously and while the flow at dropper-scale can be studied by direct numerical simulation, both larger scales need a modelled representation of the long-lines or droppers. While the main focus of this study is at the intermediate scale of a farm block, previous works at larger [Plew et al(2005)] and smaller scales [Plew et al(2009)] inspired this approach.

Large-scale interactions between a whole farm and its surrounding flow have been investigated by using scaling or numerical approaches. Large-scale models that operate at the embayment and larger scale [Panchang et al(1997), Dudley et al(2000), Cromey et al(2002), Grant and Bacher(2001), Grant et al(2008)] need to represent farms in a parameterised manner sufficiently well so as to include their influence on local circulation. This is typically achieved by some bulk drag force in a two-dimensional model [Grant and Bacher(2001), Plew(2009)]. The drag force is derived from a quadratic approximation and assumed to be due to an even distribution of drag elements (the mussel loops or "droppers'). Flow retardation depends on ambient flow speed and is statistically related to mussel rope spacing [Boyd and Heasman(1998)]. Also, dropper density and diameter (mussel-size dependent) are two key parameters to the flow reduction [Plew et al(2005)]. The whole approach, which assumes isotropic property of the whole farm as a first approximation, appears to lead to reasonable results [Plew et al(2005)].

Whereas such simple farm models are still of great interest particularly in a three-dimensional context, little is known about the influence of the positioning and orientation of long-line blocks within a farm and mussel farm flow at the intermediate scale between dropper and farm size. The highly heterogeneous properties of mussel flows combined with the parallel orientation of long-lines within each block suggest

that the drag force exerted by farm blocks and therefore the flow within a farm might be highly directional [Plew et al(2005)]. This would be consistent with the propensity of the water to choose the path of least resistance. This is notably suggested by observations by Boyd and Heasman [Boyd and Heasman(1998)] who found that water approaching a raft at an angle would still flow through the raft in a direction parallel to its short axis. However this does not mean there is not enhanced horizontal mixing affecting in/out farm exchange. On that basis, the relevance of farm block angle and the distance between farm blocks at the scale of a farm block is worth investigating.

At the dropper-scale, direct numerical simulations of two rows of ten droppers modelled as solid cylinders showed limited influence of the orientation of the long-lines onto the flow. This supports the suitability of representing a long-line as a uniform isotropic model.

This work is also of relevance to other canopy systems [Stevens et al(2008)]. Natural and man-made structural arrangements like kelp and sea grass beds [J. H. Rosman and Monismith(2007), Jackson and Winant(1983), Nepf and Koch(1999)], float breakwaters [Seymour and Hanes(1979)] and wave and offshore wind energy extraction arrays [Stevens et al(2007), Koller et al(2006)] will all influence local currents.

The present two-dimensional study is a first step towards understanding the interaction of blocks of long-lines with an upstream flow. While the flow structure within a mussel farm, and its dependence on the arrangement of the block, is interesting in itself, this type of study can help improve mussel farm models and how they can be then incorporated into larger-scale studies. The following study focuses on the two-dimensional flow past two blocks of five to ten long-lines with orientation and separation of the blocks as main parameters. Long-line blocks are represented as arrays of parallel long-lines modelled as uniform areas of enhanced friction. While the influence of the orientation and distance parameters is first investigated within a laminar uniform flow, upstream turbulence is then integrated into the model. Similar observations are made in both cases on the relevance of the orientation of the long-line blocks. Spectral analysis is undertaken to look at the turbulent structure of the flow and its evolution within the farm.

2 Model/Method

2.1 The Gerris Flow Solver

The model was setup using the Gerris Flow Solver (Gerris) [Popinet(2003)]. Gerris is a 2D/3D equation solver designed to solve the incompressible Navier-Stokes equations:

$$\begin{cases} \rho\left(\partial_t \boldsymbol{u} + \boldsymbol{u}\cdot\nabla\boldsymbol{u}\right) = -\nabla p + \nabla\cdot\left(\mu\left(\nabla\boldsymbol{u} + \nabla^t\boldsymbol{u}\right)\right) \\ \nabla\cdot\boldsymbol{u} = 0 \end{cases}$$

where $\boldsymbol{u}$ is the velocity (bold = vector), p the pressure, ρ the fluid density and μ the dynamic viscosity of the fluid. Gerris is published under the GNU General Public License and is free to download from http://gfs.sf.net. Among its many features, the code is based around a quadtree/octree finite-volume discretisation of the Navier-Stokes equations. The quadtree/octree mesh notably allows easy handling of non-uniformly refined meshes. Mesh refinement is adaptive in space and in time and can be setup using geometrical criteria as well as criteria based on the computed quantities (e.g. vorticity,

see Figure 3). This is particularly suitable to the study of multi-scale problems for which the use of an appropriate discretisation enables computational resources to be maximised [Popinet et al(2004)].

2.2 Farm block geometry

Two different types of farm blocks were used in the simulations, specifically blocks of 5 and of 10 long-lines. Whereas the 10 long-line blocks are more typical, it is expected that 5 long-line blocks are a good first approach to the problem. In both cases, the same proportions were used, with long-lines of length to width ratio of 100 and the distance between two long-lines being of 20 times the width of a long-line (Figure 2). The effective farm block geometry is slightly different from that just described as it depends on the way the ideal geometry gets discretised on the mesh, which depends on farm block position and angle. Fine resolution was applied around the long-lines (Figure 3) to ensure accurate representation of the long-lines for all configurations.

2.3 Long-line model

Following the approach of [Plew et al(2005)] at larger scale, long-lines were modelled as a uniform friction term spread over the whole rectangular long-line area. The loss of energy of the mean flow to viscous drag on a long-line is proportional to the drag force exerted by a single dropper and the dropper density within the long-line area.

The drag force due to a single dropper of length L_d and diameter ϕ [Plew et al(2005)] is given by

$$\boldsymbol{F}_d = -\frac{c_d \rho \phi L_d \, |\boldsymbol{u}|}{2} \boldsymbol{u}, \tag{1}$$

where ρ is the water density and c_d a dimensionless drag coefficient. This leads to a drag stress per grid cell that can be expressed as

$$\tau_d = -n \frac{L_d}{H} \frac{c_d \rho \phi L_d}{2} \, |\boldsymbol{u}|^2 \tag{2}$$

where n is the dropper density (number of droppers per square-metre) and H the depth of the seabed. Average dropper density for New Zealand mussel farms is estimated to be around 0.06 [Plew et al(2005)] over the whole farm. This density has to be rescaled to account for the location of all the droppers within the long-line areas. Also, as long-lines do not extend all the way to the seabed the drag stress is adjusted by a factor $\frac{L_d}{H}$. Dropper density is about ten times higher in the long-lines compared to the uniform farm approach. Assuming that the long-lines extend down to about half the water column, $n\frac{L_d}{H}$ was taken equal to 0.36.

2.4 Domain

All simulations were realized in channels with a constant inflow imposed upstream from the farms, an outflow downstream and slip boundary conditions applied to both lateral ends of the domain. In order to ensure minimum influence of the channel boundaries on the flow, a domain of size 4 km $\times$4 km was used. The ratio of the domain size to

the length of a long-line is therefore 40. Also, a coarse resolution was imposed in the region directly adjacent to the channel boundaries to dampen small-scale boundary influence. For later simulations involving turbulent inflow, the size of the domain was significantly reduced to a rectangular 800 m $\times$ 400 m. Consequently, it is possible that the borders of the channel have an influence on the mean flow. Nevertheless, given the slip boundary conditions applied on the channel wall, no production of turbulence is expected from the walls which should ensure minimum disturbance to the vortex/long-lines interaction.

2.5 Inflow velocity

It is non-trivial to recreate with great precision in a numerical model, especially in two-dimensions, flow conditions fully representative of mussel farm environment. It is clear that in reality, mussel farms are exposed to fully turbulent flows involving eddies of various size from the size of a bay to the one of the mussel themselves. Initially, farm blocks were put in a uniform and unidirectional laminar flow. From this velocity scale, V_0, a Reynolds number can be defined as

$$\mathrm{Re} = \frac{lV_0}{\nu} \tag{3}$$

where ν is the kinematic velocity of seawater and l the characteristic length-scale was chosen to be the width of a long-line.

Depending on the farm and the volume of mussel crop attached to the ropes, l usually ranges between 1 and 1.5 m. A wide variety of current flows are possible depending on location but presently farms do not tend to be placed in very strong tidal flows. Flows of 5-25 cm $.s^{-1}$ are perhaps typical [Plew et al(2005),Stevens(2003), Hartstein and Stevens(2005)]. In that context, Reynolds numbers up to 2.3×10^5 apply to mussel farm flows, with typical values between 10^5 and 1.5×10^5.

2.6 Adaptive mesh

The adaptive mesh (Figure 3) was used for two purposes :

- as stated earlier, spatial adaptivity was used to impose fine resolution ($\Delta x \sim 0.25m$) on the long-lines. Long-line refinement was kept constant during the whole simulation to allow suitable representation of the long-line geometry.
- adaptivity in time was used to resolve and follow the vortical structures forming in the wake of the long-lines. This was achieved by refining the mesh using a criterion on the vorticity (curl of the velocity field $\nabla \times \boldsymbol{u}$) with a maximum tolerance of 0.0046 s^{-1} i.e. any cell for which the vorticity is larger than 0.0046 s^{-1} was automatically refined until either the vorticity was lower than 0.0046 s^{-1} or the predefined maximum refinement level was reached. Similarly, if the local vorticity was lower than the imposed tolerance, the mesh was coarsened as long as the vorticity remained lower than 0.0046 s^{-1} or the minimum refinement level was reached. Slightly coarser mesh-refinement was used in that context with grid cells of minimum size $\Delta x \sim 1m$.

2.7 Turbulence modelling

For Reynolds numbers as high as that considered here, flows are highly turbulent with many different scales involved and several orders of magnitude separate the largest and the smallest scales of the flow. Direct numerical simulation of all scales is still far from feasible with the presently available computational resources. The simulations presented in this article ensure the resolution of the flow structures are as small as the scale of the long-lines which is far bigger than the Kolmogorov micro-scale. For that reason energy dissipation takes place at a much larger scale in the model than in reality and some modelling of the turbulent energy transfer at scales smaller than the mesh size is required [Popinet et al(2004)].

A common closure approach is to model the subgrid-scales using a space and time dependent eddy-viscosity term. Many formulations for this eddy-viscosity can be found in the literature, most of them being essentially semi-empirical relationships [Lesieur and Metais(1996)]. Because of their semi-empirical nature, these models are hard to generalise and equally good results can often be obtained using more heuristic approaches. In that respect, several studies suggest that numerical viscosity (a consequence of higher order errors associated with the discrete representation of the solution) can model turbulent subgrid energy transfer as well or sometimes better than more complex Large Eddy Simulation semi-empirical models [Popinet et al(2004)]. As a first approximation, no explicit turbulent model is used here, the implications of which will be discussed in Section 4.

A first consequence of the under-resolution of the following simulations is that the effective viscosity of the simulated fluid is mainly controlled by numerical viscosity which is hard to evaluate. In consequence, the Reynolds number of the simulation cannot rigorously be calculated from the parameters of the model. The present simulations can only be described as high Reynolds number simulations comparable with the range of Reynolds numbers found in reality.

2.8 Simple analytical model

A simple analytical model was also developed with the aim of getting a different perspective on the drag action of the long-lines to discuss the results of the computational fluid dynamics model. Let us consider a single rectangular long-line of dimension $L \times h$ and angle with the upstream flow of α (see Figure 4). An homogeneous distribution of drag is imposed on the whole long-line.

Following [Plew et al(2005)], the local loss in kinetic energy of the flow when passing through a long-line is equal to the rate of work of the long-line drag force per meter-squared. Assuming that the magnitude of the transverse flow is small compared to that of the upstream flow, we get

$$\frac{1}{2}\frac{du^2}{dt} = u\frac{du}{dt} = -C_d u^3,$$

where C_d is the drag coefficient of the long-lines in the long-lines and 0 outside.

The velocity can be determined as a function of x of the distance travelled through the farm by using $\frac{du}{dx} = \frac{1}{u}\frac{du}{dt}$ [Plew et al(2005)] which yields

$$\frac{du}{dx} = -C_d u \tag{4}$$

which can be easily solved and leads to,

$$u(x) = u_0 \exp\left(-\int_0^x C_d \,\mathrm{dx}\right). \tag{5}$$

Given this analytical description of the velocity field, the momentum loss associated with the friction exerted by a long-line can be estimated as a first approximation as:

$$\begin{array}{l} \Delta M = \rho u_0 h \cos\alpha \,(1- \exp\left(-\int_0^x C_d \,\mathrm{dx}\right)) = \rho u_0 h \cos\alpha \left(1 - \exp\left(-\frac{L}{\cos\alpha} C_d\right)\right), \\ \alpha \in \left[0 : \arctan\left(\frac{h}{L}\right)\right] \\ \Delta M = \rho u_0 L \sin\alpha \,(1- \exp\left(-\int_0^x C_d \,\mathrm{dx}\right)) = \rho u_0 L \sin\alpha \left(1 - \exp\left(-\frac{h}{\sin\alpha} C_d\right)\right), \\ \alpha \in \left[\arctan\left(\frac{h}{L}\right) : \frac{\pi}{2}\right] \end{array}$$

This analytical approach can be extended to a group of long-lines, i.e. a farm block, and the momentum loss can be evaluated by numerical integration.

While it will be shown later that this simple analytical model correlates well with the simulation results both in an intuitive and qualitative way, this description overlooks the influence of the pressure gradient existing between the upstream and downstream ends of the farm block. Indeed, due to the resistance offered by the long-lines to the flow, part of the flow's kinetic energy transforms into potential energy and a high pressure region creates upstream from the long-line leading to the establishment of a negative pressure gradient through the long-line in the flow direction. Two direct consequences of that are that the flow speed at the upstream end of the long-line is lower than far upstream and that the pressure gradient tends to accelerate the fluid in the long-lines. The pressure increase upstream from the long-line is also fundamentally related to the establishment of a transverse flow that allows part of the upstream to circumvent the long-line area (in 2D or 3D). This underlines here the fact that the continuity equation is not compatible with a one-dimensional description of the problem. Extending this analytical model to two-dimension is non-trivial and therefore the pressure term is here left aside.

3 Results

3.1 Flow past a single long-line

Figure 5 illustrates the flow past a single long-line in a laminar velocity field. The black rectangular box defines the outline of the long-line. From left to right, fluid enters the long-line zone where the friction term progressively slows it down. This results in the formation of increasingly stronger velocity gradients between the flow inside and near the long-line. Accordingly, on Figure 5, an increase in vorticity is found as the fluid moves forward in the long-line.

Whereas the flow remains laminar for the first two thirds of the long-line, perturbations appear as the vorticity gets stronger, resulting in vortex shedding within the long-line. Vortices remain at first confined to the long-line and then expand in the wake of the long-line.

3.2 Flow past two blocks of five long-lines with upstream laminar inflow

3.2.1 Setup

The first simulation setup (Figure 6) aims at investigating the angle of farm blocks with respect to the direction of the upstream flow and the distance between the two blocks as parameters to the flow through two blocks made of five long-lines each. The upstream flow is laminar and is not varied between simulations. The importance of the angles (α_1, α_2) and the distance d between the centre of two farm blocks are investigated separately.

Simulations were conducted for various combinations of the angles (α_1, α_2) and d. Among the many outputs offered by the model (instantaneous and mean velocity field or transects, vorticity), the vorticity field was found to be the most relevant and is used to illustrate the behaviour of the model.

3.2.2 Influence of the orientation of the farm blocks

For most simulations, the generation of turbulence by the time the flow exits the second farm block was observed. Turbulence is generated at the scale of the long-lines due to the gradient of velocity between the fluid inside the long-lines and the fluid outside the long-lines. This results usually in the formation of coherent vortex streets that can interact with each others depending on the angle of the farm (see Figure 7).

The transition to turbulence is very sensitive to the angles of the farm blocks (α_1, α_2). The closer the angle is to the mean flow direction, the quicker the flow will become turbulent. When the first farm makes an angle of 5 degrees with the mean flow direction the flow becomes turbulent in the wake of the first farm (Figure 7-a), when the angle is of 7 degrees the flow becomes turbulent in the wake of the second farm (Figure 7-b) and when the angle is of 13 degrees (Figure 7-c) it does not fully become turbulent within the simulation domain.

Two main factors were identified as being key to the generation of strong velocity gradients and to the transition to turbulence :

- the strength of the velocity gradient created by the drag action of a whole long-line is directly related to the angle between the long-line and the direction of the upstream flow. When long-line and upstream flow are aligned, only a small fraction of the upstream fluid goes through the long-line and this small fraction gets significantly slowed down which results in the creation of strong velocity gradients. Conversely, if the long-line is perpendicular to the flow, its dampening action is more spread out resulting in lower generation of vorticity.
- the sensitivity to the angle is also closely related to whether or not part of the fluid can go through a farm block without entering the long-lines. This creates stronger local velocity gradients and therefore more vorticity

For small values of α_1 or α_2 (i.e. $\leqslant O(10)$), high sensitivity of the flow to the angles is found whereas for higher value, it remains mostly laminar and no other flow pattern develops. This is related to the previously cited factors and whether the flow crosses the long-line in the length or the width of the long-line.

Observation of the mean velocity field (Figure 11) shows a clear reduction of the mean flow intensity of up to 20% in the wake of the farm blocks. Nevertheless, no outstanding large-scale pattern was found at the scale of a farm block.

3.2.3 Influence of the distance between farm blocks

The distance between two farm blocks does not have a major influence on the flow, at least in the range of parameters usually met in reality. Similar flows were found when the distance between the two farm blocks was varied for constant values of α_1 and α_2 (see Figure 8). Very little was observed from velocity transects of the whole domain which are therefore not presented here. The model predicts that variation of the distance between farm blocks does not affect the way the flow is "recovering" from crossing through a farm block.

It is premature to assert that the structure of the turbulence is unaffected by the distance between two farms but no variation in the size of the coherent eddies has been observed on the vorticity plots. In all cases, the mean flow remains uni-directional. No noteworthy transverse mean flow can be observed in the gap between the farm blocks.

3.3 Flow past two blocks of ten long-lines in a turbulent flow

3.3.1 Setup

The second model configuration involves two main changes. Ten long-lines are used per farm block instead of five previously. This is more similar to farm block configurations found in reality. Also, turbulence is generated upstream from a fictitious farm block.

While it is clear that the flow upstream from the farm should be fully turbulent, the upstream size of the eddies containing the most energy is case-dependent and generating a relevant upstream turbulence is non-trivial and beyond the scope of this study. This approach to turbulence generation using a fictitious farm block allows generation of coherent turbulent eddies within a limited frequency band. Rescaling of the farm block allows generation of smaller or larger structures. Also, it is likely that such eddies are representative of part of the turbulence spectrum that can be found within a mussel farm.

3.3.2 Influence of the angle

As for the laminar flow experiments (section 3.2), several simulations were run for a similar upstream flow regime and different angles of the farm blocks with the mean upstream velocity. Those simulations led to conclusions similar to the ones previously established. For small angles (Figure 10-a), strong interactions are observed between long-lines and surrounding flow. This results in bands of high vorticity which make the long-line zones apparent in the vorticity field plots.

For high farm block angles (Figure 10-b), little interaction is found between long-lines and flow. It is not obvious from the vorticity plots whether the structure of the turbulent wake is affected at all. Similarly, no obvious vorticity damping is found in the second farm.

Those observations corroborate the conclusion of the laminar model. For small angles, turbulence is generated at the scale of the long-lines which should enhance mixing. Conversely, for large angles, the flow is barely changed by long-lines.

3.3.3 Mean flow reduction

The mean flow reduction was calculated from time-averages of the velocity field over several times the vortex-shedding period of the long-lines (see Figure 11). The mean flow reduction within the farm blocks is complex and highly dependent on the position of the two farm blocks and of the upstream fictitious block. Nevertheless, the mean flow reduction in the wake of the farm is found to be fairly homogeneously distributed. Also, for the range of parameters studied here, no significant difference in the magnitude of the mean flow reduction is noticeable. However, because of the aspect ratio of the farm blocks, the second farm block has an influence only on half of the wake of the first farm.

3.3.4 Mixing and residence time

A measure of the residence time of fluid within a farm block provides a different point of view on turbulence and mixing. The residence time is defined here as the time spent by a small volume of fluid within the long-lines. In the context of mussel farms, it can be seen as representative of the depletion in nutrients of a small volume of fluid or to its concentration of waste produced by the mussels.

The residence time is generated by initially associating the long-line volume with a source of tracer constant in time. This tracer is advected by the velocity field and gets eventually dispersed by turbulence. The total residence time over the simulation domain is more or less constant and configuration-independent. In consequence, the main interest of these outputs are the maxima in residence time and the way residence time spreads out from the long-lines to the rest of the domain.

The maxima in residence time are found at very localised places within the long-lines, essentially within or in the direct proximity of the long-lines which corresponds to the location of the "sources of residence time" in the model. The locations of these maxima vary with time but remain always confined to the long-line area. These observations stand for the farm blocks with small angles α_1 or α_2 whereas for larger angles the residence time grows more uniformly in space and no noticeable extrema is found.

The downstream distribution of residence time is found to be angle-dependent, or, it would be more appropriate to call it aspect ratio-dependent. Figure 12-c illustrates well this aspect ratio-dependence. In the case of a farm block of aspect ratio 1, then it is really angle-independent. In all cases, the far downstream wake of the farm is close to present a uniform distribution of residence time.

Interestingly, while the angles of the farm blocks have a strong influence on the production of vorticity and mixing, they do not have a major impact on the dispersion of waste or depletion of nutrient at the scale of the farm, at least for farms made of a limited number of farm blocks. For small angles, the very inhomogeneous initial distribution of residence time is counterbalanced by the mixing produced by the interaction of the long-lines with the mean flow and *vice versa*.

No major difference is found when the scale of the upstream vortices is varied. Nevertheless, it is clear that a large part of the upstream turbulence survives the crossing of the long-lines blocks and therefore plays a role in the transport of residence time. As stated earlier, many scales of variability are not included in the model and turbulence intensity is more likely to be underestimated in the model than the opposite. However, this model assumes the water goes through 2 farm blocks at most and it could be much more in reality (see Figure 15). When the flow reduction caused by the

successive crossing of farm blocks becomes too important, it is conceivable that mixing efficiency changes and that some farm blocks arrangements are better than others.

3.4 Aerial observation

No attempt is made in this study to simulate measurements made on real mussel farms. Nevertheless, the aerial views of a mussel farm presented in Figure 13 are of interest. Strong resemblances are found between the photographed wake and the wake structure predicted by the numerical model (see Figure 12). The upstream flow direction in the photograph is slightly different to the one on Figure 12, but a fairly homogeneous wake with hints of the presence of vortical structures can be observed. The main difference lies in the central part of the wake where a band of much lighter colour is observed. This is likely due to the fact that the fifth long-line from the left seem thinner than the other ones and would therefore make a smaller contribution to the wake.

3.5 Simple analytical model

Numerical integrations of the simple analytical model were performed for the flow past a single farm block. Dimensions similar to the ones used in the computational fluid dynamics model are used here. Farm blocks made of 4 to 16 long-lines and of angles with the upstream flow of 0 to 90 degrees were used. The flow velocity upstream from the farm was taken to be equal to 1 $m.s^{-1}$.

The aim of this model is to give a simple perspective on the influence of farm block angle and of the number of long-lines per farm blocks on mean flow reduction and vorticity production created by flow/long-line interactions. Mean flow reduction is believed to scale with the integral of the flow reduction over the wake on the farm block. Vorticity production is related to velocity gradients and should scale with the maximum local flow reduction in the wake of a farm block or with the difference between the local maximum and the local minimum in the wake of a farm block.

Total mean flow reduction (Figure 14-a) is found to be angle-dependent for small angles and mostly angle-independent for larger angles of 10 to 90 degrees. Total mean flow reduction increases quickly with the angle for angles of 0 to 10 degrees and then remains more or less stable except when the number of long lines per farm block is more than 10. When more than 10 long lines per farm block are used, flow reduction decreases slightly for angles of 50 to 90 degrees. The small flow reduction for angles smaller than 10 degrees is directly related to the laminar flow envisaged here. Indeed, from equation 2.8, local flow reduction is directly proportional to upstream flow intensity and for long-lines quasi-aligned with upstream flow direction, flow reduction diminishes quickly as fluid goes through the long-line. Such effects would be limited in the presence of horizontal mixing and therefore as a first approximation the simple model seems to indicate that mean flow reduction is close to being angle-independent and is quasi-proportional to the number of long-lines per farm block.

Difference between local maxima and minima in flow reduction in the core of the farm's wake (Figure 14-b) with which vorticity production should scale, is found to be completely independent of the number of long-lines of the studied farm block. Again, the results can be split in between small angles (0 to 10 degrees) and large angles (10 to 90 degrees). Small angles are associated with large velocity gradients. Those are

strongly sensitive to the angle between the long-lines and the upstream flow direction and decrease quickly when the angle is increased. Conversely, relatively small velocity gradients are associated with larger angles.

4 Discussion

4.1 Upstream mixing

No particular differences were found in the way long-lines interact with their surrounding flow between simulations with laminar and turbulent upstream flows. However, it appears that upstream mixing is not dampened and plays a major role through the crossing of the whole farm. While flow/long-line interactions generate vorticity near and within the long-lines, this vorticity allows efficient mixing only in the wake of the long-lines. The efficiency of the mixing within a farm block is therefore essentially related to upstream turbulence. In that respect, block arrangement in a farm can be of great importance with blocks interacting with each other.

Upstream mixing here is ensured through the use of a fictitious farm block which sheds vortices on the studied farm blocks. Despite the different sizes examined here, the upstream mixing corresponds to the turbulent wake behind a farm block. A very limited range of turbulent eddies is therefore present compared to what is found in reality. Also, turbulent energy in the upstream flow is likely to be much higher in reality due to the presence of gravity waves, variability in coastal circulation and of a benthic boundary layer. In consequence, efficient mixing of the waste produced by mussels and of the nutrient supply should be ensured for mussel farms.

4.2 Mussel-farm modelling at larger scale

The presence of long-lines affects the environment in three different ways. First, the drag force of the long-lines on the passing fluid induces energy dissipation which results in the reduction of the magnitude of the mean flow. Secondly, this drag effect creates velocity gradients in the vicinity of the long-lines. In those regions of high shear stresses, vorticity is produced corresponding to the transformation of part of the kinetic energy of the flow into turbulent kinetic energy. Finally, from a non-hydrodynamical point of view, mussels are living organisms and their presence is accompanied by the production of waste (faeces and pseudo-faeces) and the consumption of nutrient (seston). Ideally, a mussel farm model should represent all of those three processes.

The present model goes down to scales close to those of the objects generating friction and waste or nutrient depletion. For that reason, provided adequate calibration, such a model should lead to a relatively good representation of the reality. Any larger-scale model of a mussel farm would involve the representation of a much more heterogeneous system with highly directional properties. While it was initially undertaken to study mussel farm flow dynamics at the scale of several farm blocks, given the limited relevant observations made on farm-block size flow, most conclusions on mussel farm model improvement address the scale of a farm-block more so than that of a whole farm.

A strong influence of the farm angle on the long-line vorticity production was found from the first set of simulations with laminar upstream flow. While in that case,

the angle of the farm was also controlling the structure of the wake behind the farm block, those observations are nuanced by the second set of simulations with upstream turbulence. The importance of the farm block angle for the generation of vorticity is confirmed, which is not the case for the structure of the wake. The presence of upstream turbulence has a strong impact on the homogenisation of the long-line scale properties of the flow, and regardless of the angles of the farm-blocks, the distributions of vorticity as well as the ones of residence time are fairly uniform. The study of the mean velocity field is also in agreement with those observations and display comparable mean-flow reductions for farm block at angle 0 or 90 with the upstream flow.

The present model is two-dimensional and only involves a single set of parameters for the flow Reynolds number and the drag associated with the long-line. This suggests that the changes in mean flow direction that has been measured in some case in the wake of mussel-farms [Plew et al(2005)] are not controlled at the scale of the farm-blocks, and therefore might be dependent on the arrangements of the farm blocks within the farm. It would nevertheless be of interest to consider higher values for the friction coefficient associated with the long-lines to confirm those observation in the case of a system more strongly constrained by the long-lines. If the observations remain the same, then long-lines blocks can be modelled as isotropic, i.e angle-independent, uniform drag elements and nutrient sinks or waste sources. The second point that could be considered is to superimpose a vorticity or turbulent kinetic energy source term to the drag term, which this time would be angle-dependent.

As showed by the analytical model, mean drag is essentially proportional to the surface area occupied by the long-lines and proportional to it. Vorticity production is proportional to the shear created by the friction effect of the long-lines which is clearly angle-dependent and scales with the drag coefficient of the long-lines and the length of the largest streamwise crossection of the longlines. For small angles, the cross section is large, and vorticity generation is large whereas for angles between 10 to 90 degrees the size of the long-line cross-section is minimised and little vorticity is generated.

Provided efficient mixing and no food limitation for the mussels, nutrient/waste sink and source are *a priori* uniform and constant and residence time can be modelled as a uniform source. When it comes to waste production, the sinking speed of the waste should be taken into account [Giles and Pilditch(2004)] and waste with large sinking speed might not get mixed that efficiently.

4.3 Future work

The model presented in this article takes advantage of the adaptive mesh-structure of the Gerris Flow Solver to provide high resolution simulations of the flow past two mussel farm blocks. Clear trends have been identified regarding the influence of the long-lines angle on the mean drag, vorticity and mixing production. These observations were explained with the help of an analytical model. Spectral analysis of the flow within the farm-blocks provided limited information but illustrated well the degree of spatial and temporal variability involved in such flows.

This work provides motivation for new observations on the decameter-scale variability. Traditionally coastal oceanography has sought to characterise the coastal circulation scale and the dissipation scale where energy is lost. Spatio-temporal variability at the scale induced here is not a common focus. This is not surprising as there are not many forcing situations other than canopy structures that produce this. Areas for

future emphasis include the step to 3D, the inclusion of a closure scheme and a variable boundary-flow to simulate variability in coastal flows. Also, it would be of interest to consider different values for the friction coefficient associated with long-lines to confirm the present results.

Acknowledgements The authors are grateful to to Dr. D. Plew for commenting this manuscript and to Dr. Barb Hayden for leading and helping in this project. This work was funded by the sustainable aquaculture programme of the New Zealand Foundation for Research, Science and Technology and the Marsden fund of the New Zealand Royal Society.

References

[Blanco et al(1996)] Blanco J, Zapata M, Morono A (1996) Some aspects of the water flow through mussel rafts. Scientia Marina 60(2-3):275–282

[Boyd and Heasman(1998)] Boyd AJ, Heasman KG (1998) Shellfish mariculture in the benguela system: water flow patterns within a mussel farm in Saldanha Bay, South Africa. Journal of Shellfish Research 17(1):25–32

[C. A. Pilditch and Bryan(2001)] C A Pilditch JG, Bryan KR (2001) Seston supply to sea scallops (placopecten magellanicus) in suspended culture. Canadian Journal of Fisheries and Aquatic Sciences 58:241–253

[Cromey et al(2002)] Cromey CJ, Nickell TD, Black KD (2002) Depomod - modelling the deposition and biological effects of waste solids from marine cage farms. Aquaculture 214:211–239

[Dudley et al(2000)] Dudley RW, Panchang VG, Newell CR (2000) Application of a comprehensive modeling strategy for the management of net-pen aquaculture waste transport. Aquaculture 187(3-4):319–349

[Giles and Pilditch(2004)] Giles H, Pilditch CA (2004) Effects of diet on sinking rates and erosion thresholds of mussel perna canaliculus biodeposits. Marine Ecology Progress Series 282:205–219

[Grant and Bacher(2001)] Grant J, Bacher C (2001) A numerical model of flow modification induced by suspended aquaculture in a Chinese bay. Canadian Journal of Fisheries and Aquatic Sciences 58:1003–1011

[Grant et al(2008)] Grant J, Bacher C, Cranford PJ, Guyondet T, Carreau M (2008) A spatially explicit ecosystem model of seston depletion in dense mussel culture. Journal Marime System 73(1-2):155–168

[Hartstein and Stevens(2005)] Hartstein ND, Stevens CL (2005) Deposition beneath long-line mussel farms. Aquacultural Engineering 33:192–213

[J. H. Rosman and Monismith(2007)] J H Rosman JRK, Monismith SG (2007) A field investigation into the effects of a kelp forest (macrocystis pyfera) on coastal hydrodynamics and transport. Journal of Geophysical Research 112:CO2016

[Jackson and Winant(1983)] Jackson GA, Winant CD (1983) Effect of a kelp forest on coastal currents. Continental Shelf Research 2:75–80

[Koller et al(2006)] Koller J, Koppel J, Petters W (2006) Offshore Wind Energy - Research on Environmental Impacts. Springer

[Lesieur and Metais(1996)] Lesieur M, Metais O (1996) New trends in large-eddy simulation of turbulence. Annual Review of Fluid Mechanics 28:45–82

[Nepf and Koch(1999)] Nepf H, Koch E (1999) Vertical secondary flows in submersed plant-like arrays. Limnology and Oceanography 44(4):1072–1080

[Panchang et al(1997)] Panchang VG, Cheng G, Newell CR (1997) Modeling hydrodynamics and aquaculture waste transport in coastal maine. Estuaries and Coasts 20(1):14–41

[Plew et al(2005)] Plew D, Stevens CL, Spigel RH, Hartstein ND (2005) Hydrodynamic implications of large offshore mussel farms. IEEE Jouornal of Oceanic Engineering 30(1):95–108

[Plew(2005)] Plew DR (2005) The hydrodynamic effects of long-line mussel farms. PhD Thesis Department of Civil Engineering, University of Canterbury. digital-library.canterbury.ac.nz/data/collection3/etd/adt%2DNZCU20060106.144622

[Plew(2009)] Plew DR (2009) Drag coefficients for modelling flow through suspended canopies. Submitted to Journal of Marine Ecology

[Plew et al(2009)] Plew DR, Enright MP, Nokes RI, Dumas JK (2009) Effect of mussel biopumping on the drag on and flow around a mussel crop rope. Aquacultural Engineering 40:51–61

[Popinet(2003)] Popinet S (2003) Gerris: a tree-based adaptive solver for the incompressible Euler equations in complex geometries. Journal of Computational Physics 190:572–600

[Popinet et al(2004)] Popinet S, Smith M, Stevens CL (2004) Experimental and numerical study of the turbulence characteristics of air flow around a research vessel. Journal of Ocean and Atmosphere Technology 21(10):1574–1589

[Seymour and Hanes(1979)] Seymour RJ, Hanes DM (1979) Performance analysis of tethered float breakwaters. J Waterway, Port, Coastal and Ocean Engineering 105(3):265–280

[Stevens et al(2007)] Stevens C, Smith M, Gorman R, Popinet S, Walters R (2007) Marine renewable energy research in New Zealand: A multi-scale perspective of resources and impacts. Australian Coasts and Ports Conference, Melbourne Australia

[Stevens(2003)] Stevens CL (2003) Turbulence in an estuarine embayment: observations from Beatrix Bay, New Zealand. Journal of Geophysical Research 108:10.1029/2001JC001221

[Stevens et al(2008)] Stevens CL, Plew D, Hartstein N, Fredriksson D (2008) The physics of open-water shellfish aquaculture. Aquacultural Engineering 38(3):145–160

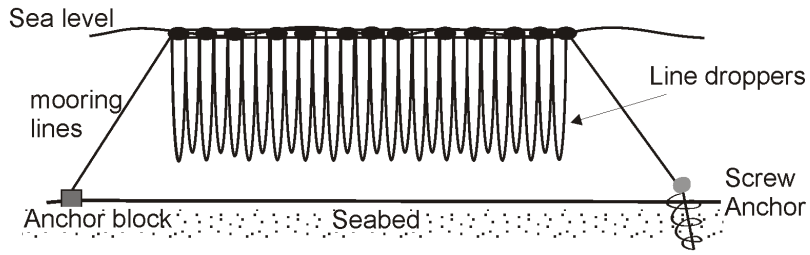

Fig. 1 Sketch of a long-line after [Plew et al(2005)].

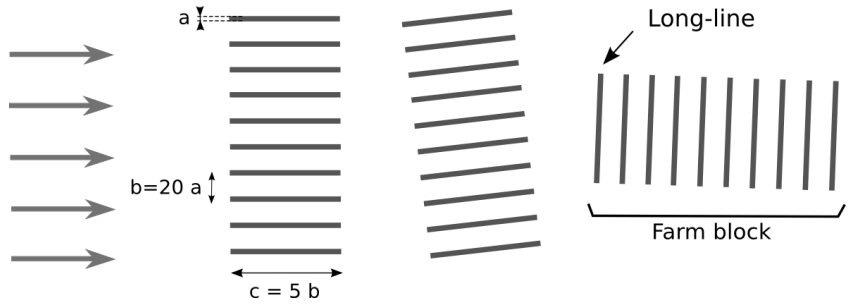

Fig. 2 Example of mussel farm configuration. Mussel farms are usually made of at least 20 farm blocks. Typical values for a,b and c are 2, 25 and 120 metres.

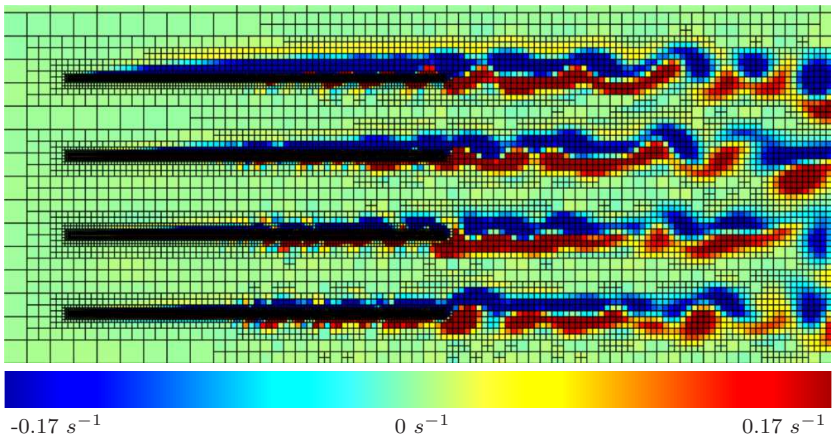

Fig. 3 Adaptive mesh near long-lines. Fine resolution of the long-lines allows accurate representation of the long-line area where the drag term corresponding to the mussel 'droppers' is applied. Vortical structures generated by the long-lines are "followed" by the adaptive grid.

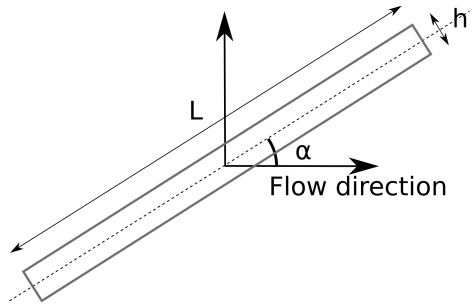

Fig. 4 Schematic representation of a long-line as used in the simple analytical model.

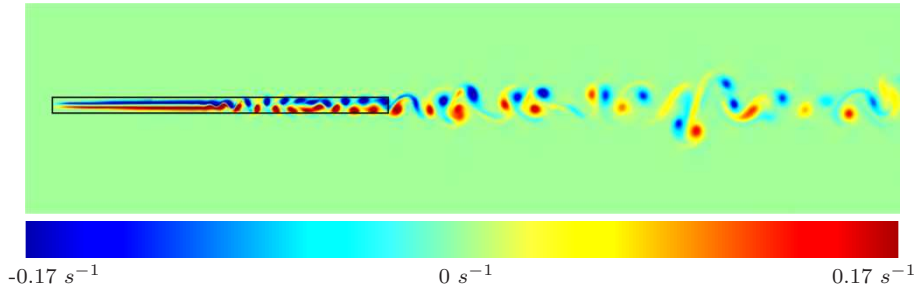

Fig. 5 Flow past a single long-line parallel to the mean flow direction. The shear caused by the long-line induces vortex shedding in the wake of the long-line. Vortices are forming within the long-line and then expelled in the wake.

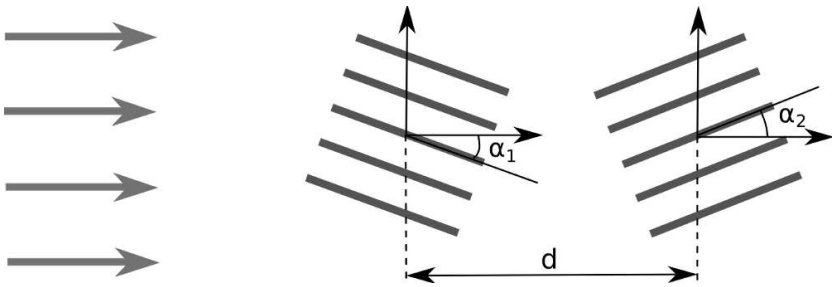

Fig. 6 The first set of simulations was realized using 2 farm blocks of 5 long-lines in a laminar flow. The 3 parameters of the simulation are the distance between both farm blocks, d, and the angle between each farm block and the inflow direction, α_1 and α_2.

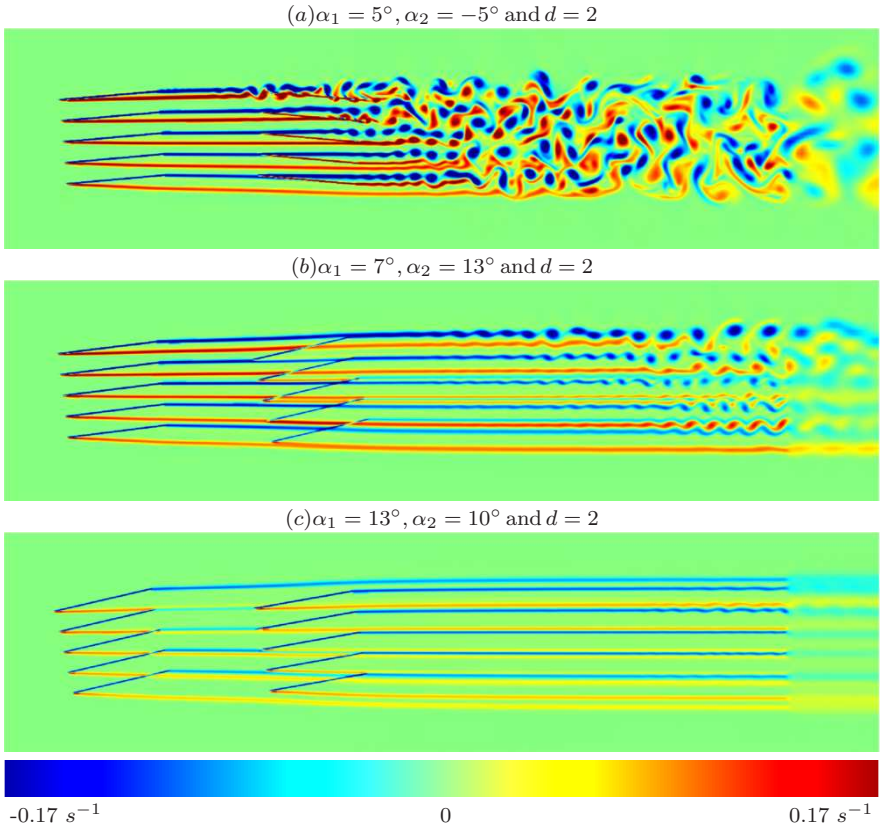

Fig. 7 Established vorticity field for three different orientations of the farm blocks. The distance d between the centre of the two blocks is normalised by the size of a long-line. The same orientation is kept between the farm blocks for all three simulations.

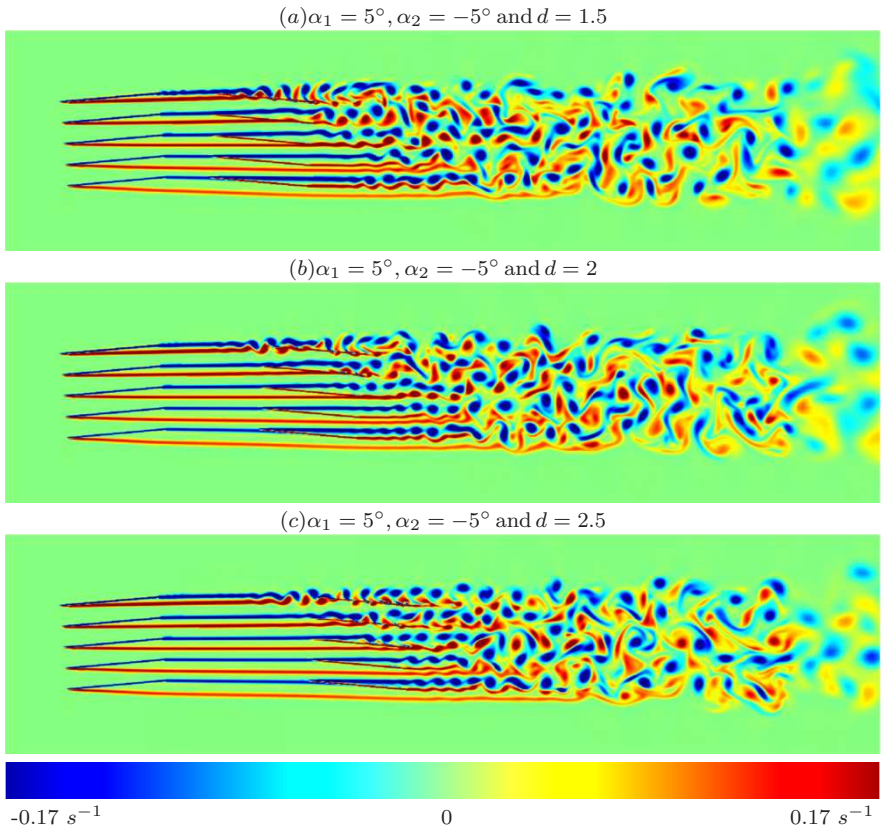

Fig. 8 Established vorticity field for three different distances between the farm blocks. The distance d between the centre of the two blocks is normalised by the size of a long-line. The same orientation is kept for the farm blocks for all three simulations.

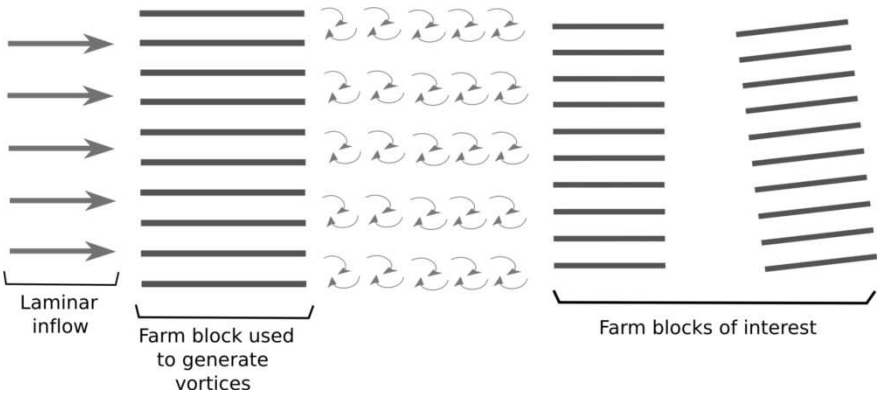

Fig. 9 A first farm block is used to generate vortices in order to expose the downstream farm blocks to a turbulent flow. The scaling of the first farm block was varied to change the size of the upstream coherent structures.

$(a)\alpha_1 = 0°, \alpha_2 = -7°, d = 1.75$ and upstream farm scale = 1

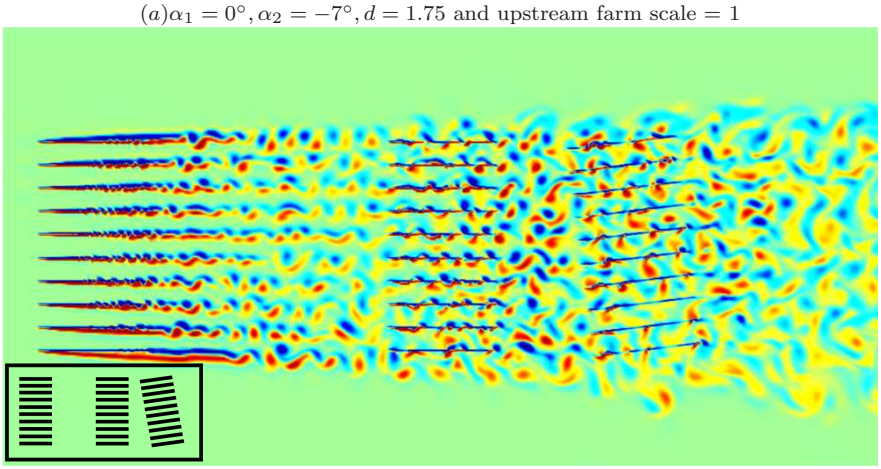

$(b)\alpha_1 = 0°, \alpha_2 = 90°, d = 1.75$ and upstream farm scale = 1

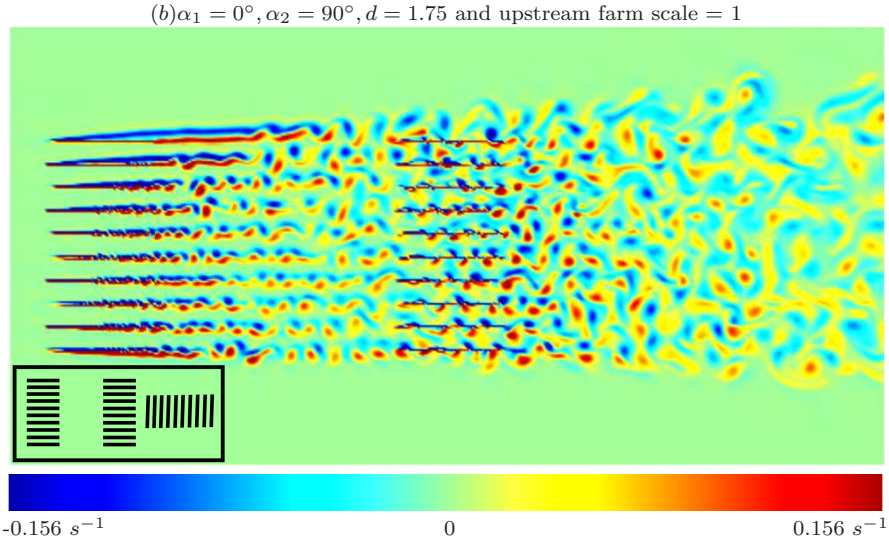

-0.156 s^{-1} 0 0.156 s^{-1}

Fig. 10 Vorticity field for a turbulent flow past two farm blocks at angles (α_1, $\alpha 2$) = (0, 7) (top) and (0, 90) (bottom). The importance of the angle between flow direction and farm is neat with the long-lines being regions of high vorticity for small angle (top) and almost no interaction noticeable for large angles (farm 2 - bottom).

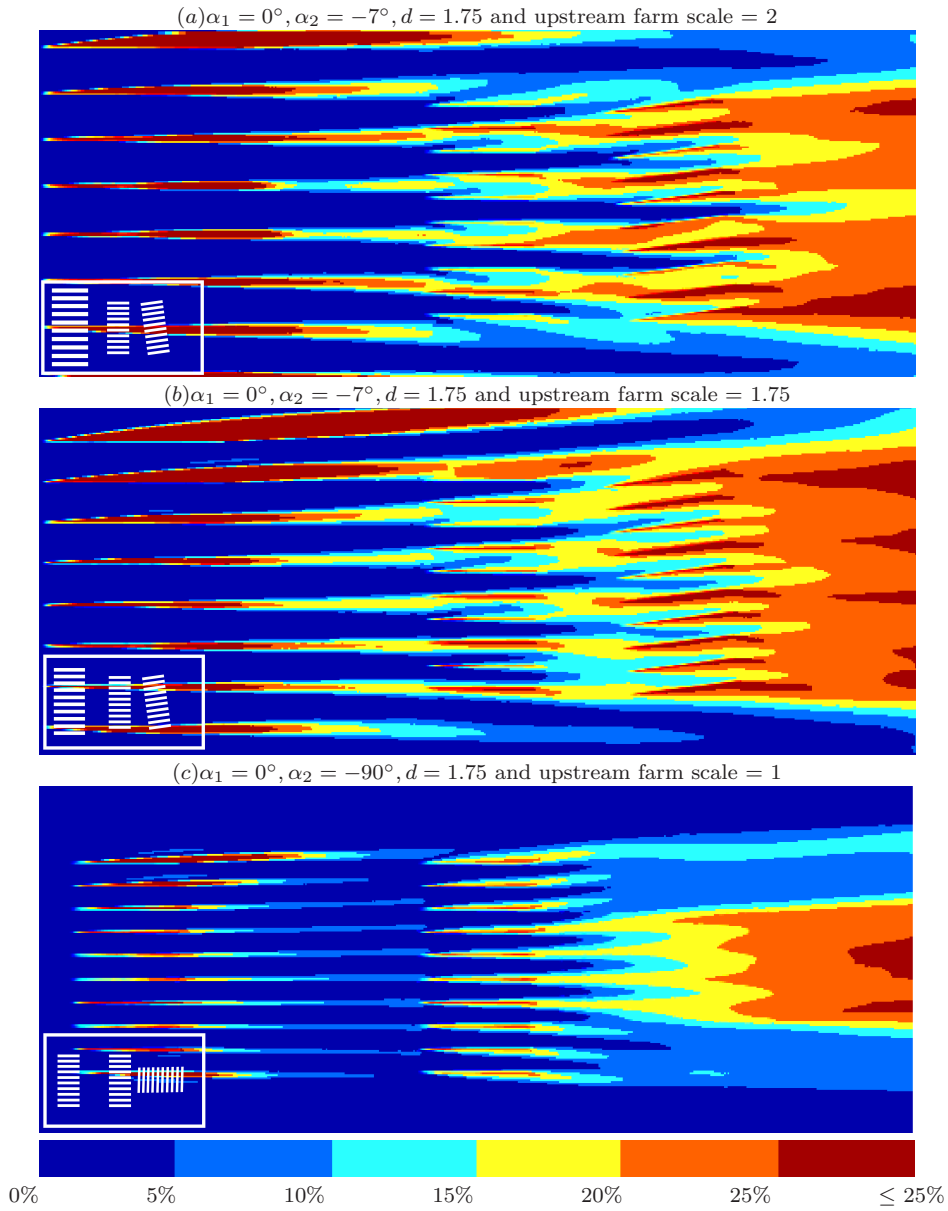

Fig. 11 Mean flow reduction in percent. The mean flow reduction in the wake of the farm blocks is mainly dependant of the aspect ratio of the farm blocks.

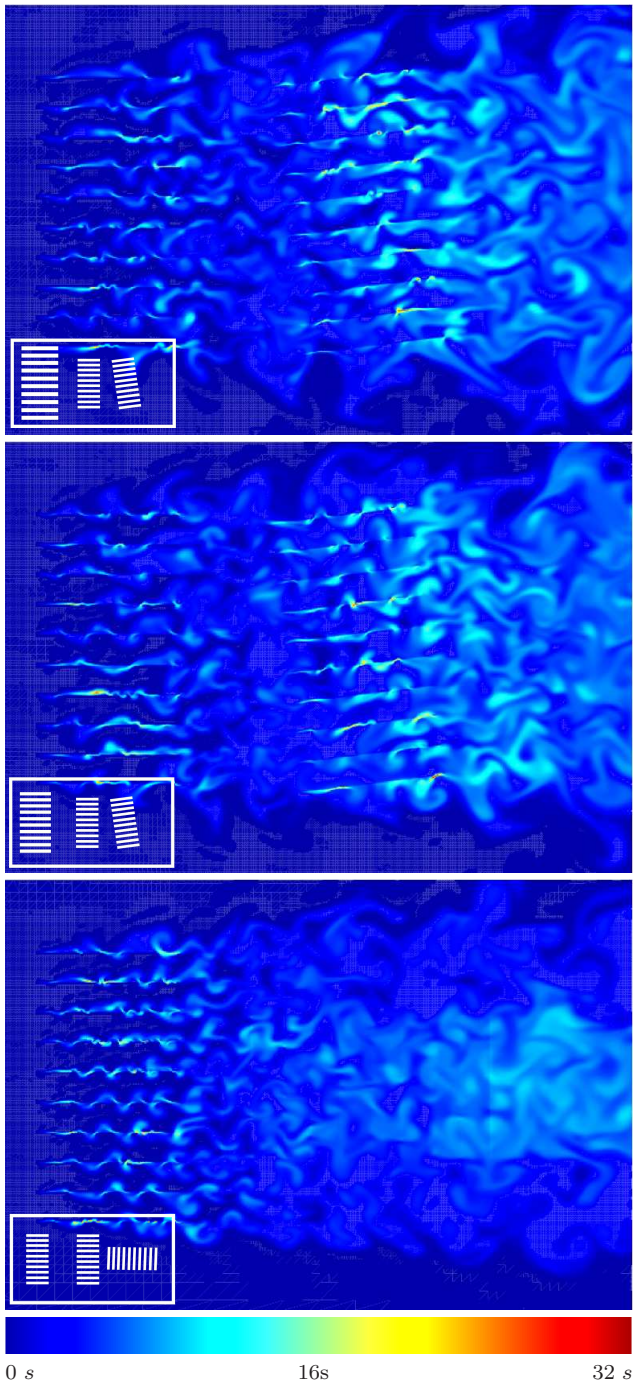

Fig. 12 Fluid residence time for three different configurations. The same color scale is used for all of the plots.

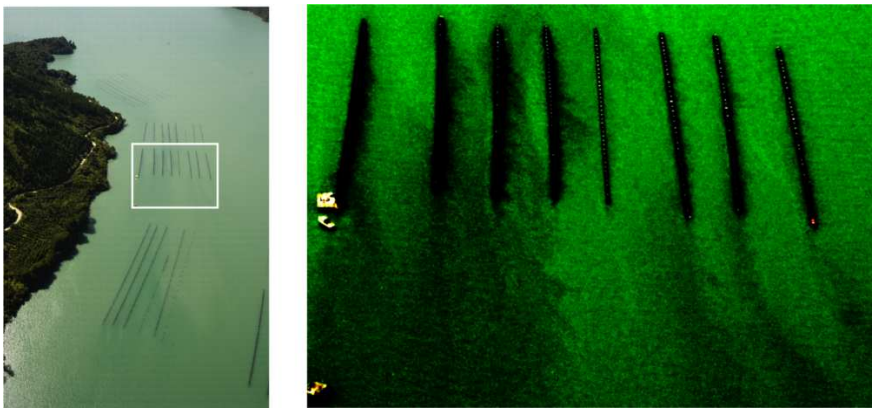

Fig. 13 Aerial photography of long-lines in the Marlborough sounds (New Zealand). The right hand panel is a zoom on the rectangular area of the left hand original photograph. Colors have been enhanced for the right hand panel. Structures similar to the wakes found in the numerical simulations can be observed on the right hand picture. Photograph: Alan Blacklock

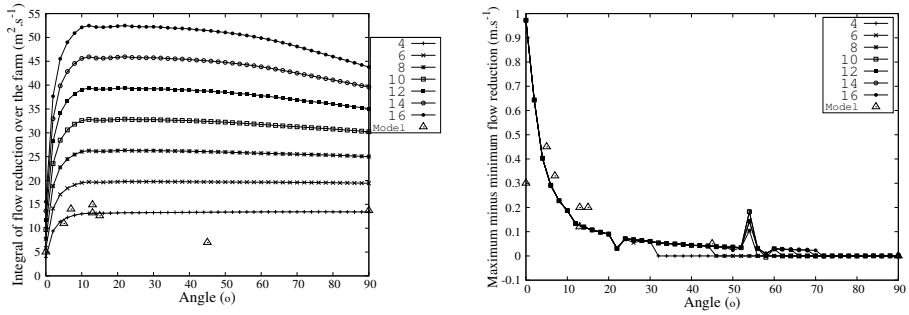

(a) (b)

Fig. 14 Results from the "simple model". (a) Integral of the reduction in velocity over the wake behind a farm block versus farm block angle for blocks made of 4 to 16 long lines. (b) Difference between the local maximum and minimum reduction in flow in the wake behind a farm block versus farm block angle for blocks made of 4 to 16 long lines. The triangular points labelled "model" correspond to the simulation made using the Gerris Flow Solver. The peak at 52 ○ is a numerical artefact.

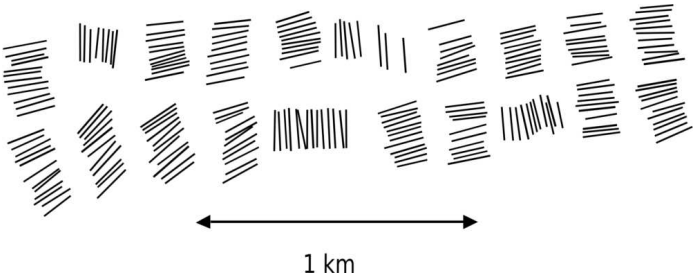

Fig. 15 Example of farm arrangement as found in reality after [Plew et al(2005)].